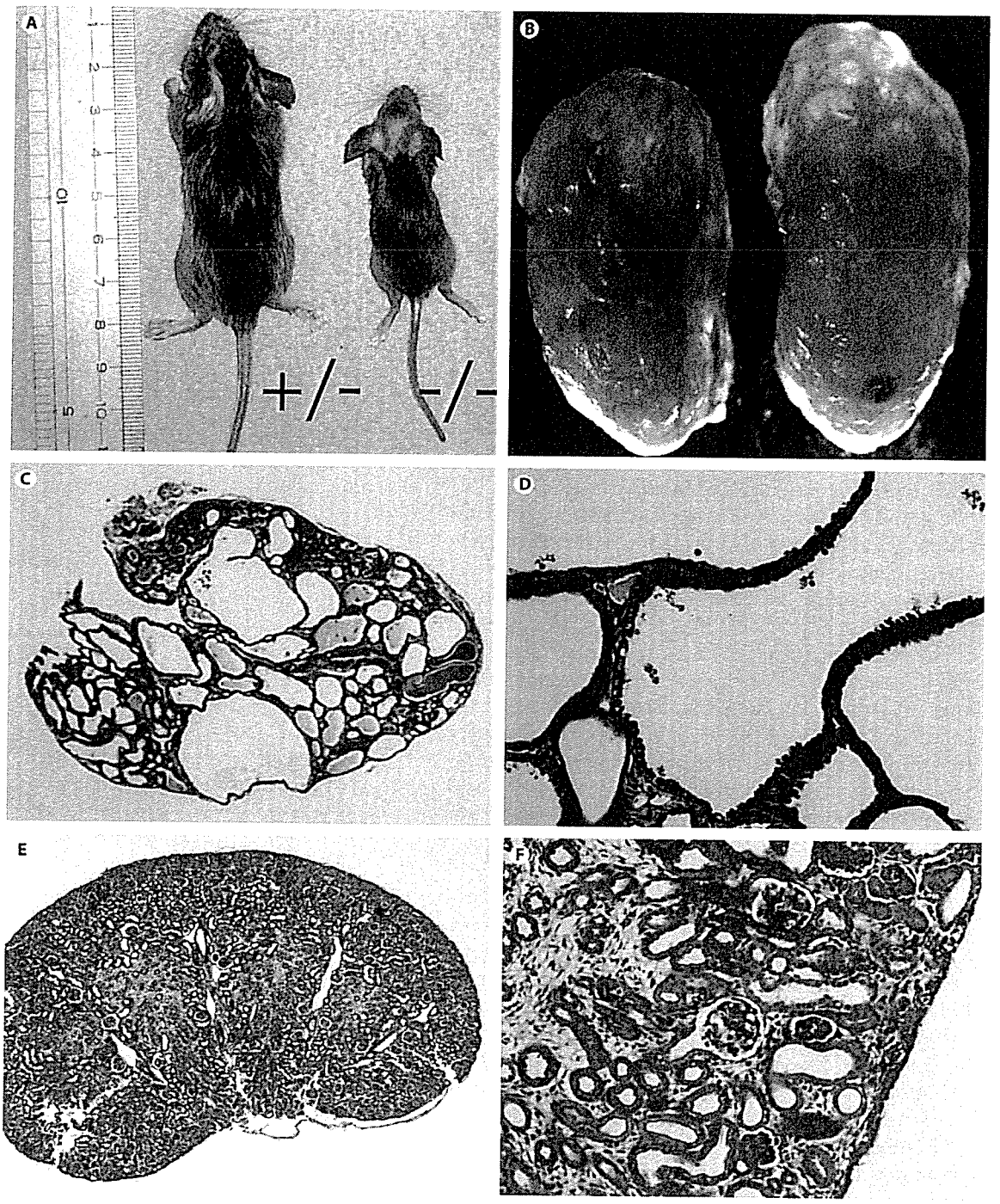

Fig. 4. Only one *Lgr4* null mouse of 667 littermates survived for 42 days. **A** Body length and appearance of a heterozygous mouse and its null littermate were compared at P28. **B** The kidney of the long-surviving null mouse is shown. The kidney was entirely swollen at the time of death with multiple cysts. Hematoxylin-eosin stains on kidney sections from P42 null and wild-type littermates. **C–F** Cysts are present in the kidneys of the null mouse (**C**, **D**), whereas the kidneys of a wild-type littermate mouse (**E**, **F**) appeared normal.

As illustrated in figure 5B, the sizes of kidneys of *Lgr4* null mice are significantly smaller than those of wild-type (and heterozygous; data not shown) littermates (fig. 5A), indicating renal hypoplasia. Spectrums of gross pathologies were appreciated in evaluating the gene-manipulated mice. Some showed hypoplastic kidneys with polycystic changes (fig. 5B, left kidney).

To assess renal function, plasma creatinine levels [14] were measured in *Lgr4* mutant and wild-type mice at birth (P0). As shown in figure 5C, a significant elevation in plasma creatinine levels can be observed in *Lgr4* null mice compared to wild-type mice at this early time point, demonstrating a lack of efficient clearance by the kidneys in *Lgr4* mutants. It is also important to note that the smaller $Lgr4^{-/-}$ animals have lesser muscle mass to contribute to a creatinine load, and so plasma creatinine levels alone, while instructive, likely underestimate compromises of their glomerular and tubular function.

Figure 6A–F show the histological findings of kidneys in wild-type and *Lgr4* null mice at birth (P0). Besides the overall size reduction (fig. 6B), kidneys from *Lgr4* null mice show significant reductions in glomerular and tubular numbers and density (fig. 6E, 7) compared to those of wild-type mice (fig. 6D, 7). In more than half of *Lgr4* null mice at birth, however, the basic structure of an individual glomerulus or tubule is maintained (fig. 6E). Some *Lgr4* null mice with high plasma creatinine levels at birth (P0) showed renal hypoplasia (fig. 6C) and absence of functional nephrons (fig. 6F). In several *Lgr4* null mice, more subtle asymmetries between the left and right kidneys (fig. 6G) were noted, with no differences in close histology (fig. 6H).

Given the reduced kidney sizes and elevated plasma creatinine concentrations seen, we suspected decreases in the number of functional nephrons in *Lgr4* null mice. Glomerular counting showed insufficient numbers of nephrons in these mice reflective of both kidney size and reduced glomerular density. Figure 7 indicates decreased total numbers of nephrons per unit area, suggesting that LGR4 contributes directly or indirectly to normal nephron density in the kidney (see Discussion).

To study any effects of *Lgr4* gene deficit on ureteric bud branching, the kidneys of E13.5 mice were histologically analyzed. Kidney samples from E13.5 wild-type (fig. 8A, C) and null (fig. 8B, D) embryos showed no obvious difference in their ureteric bud branching. In addition, a similar density of the ureteric bud tip was observed with both kidneys from wild-type and null mice (fig. 8E). These data imply that the *Lgr4* gene is more important to the development and maintenance of the glomerulus in

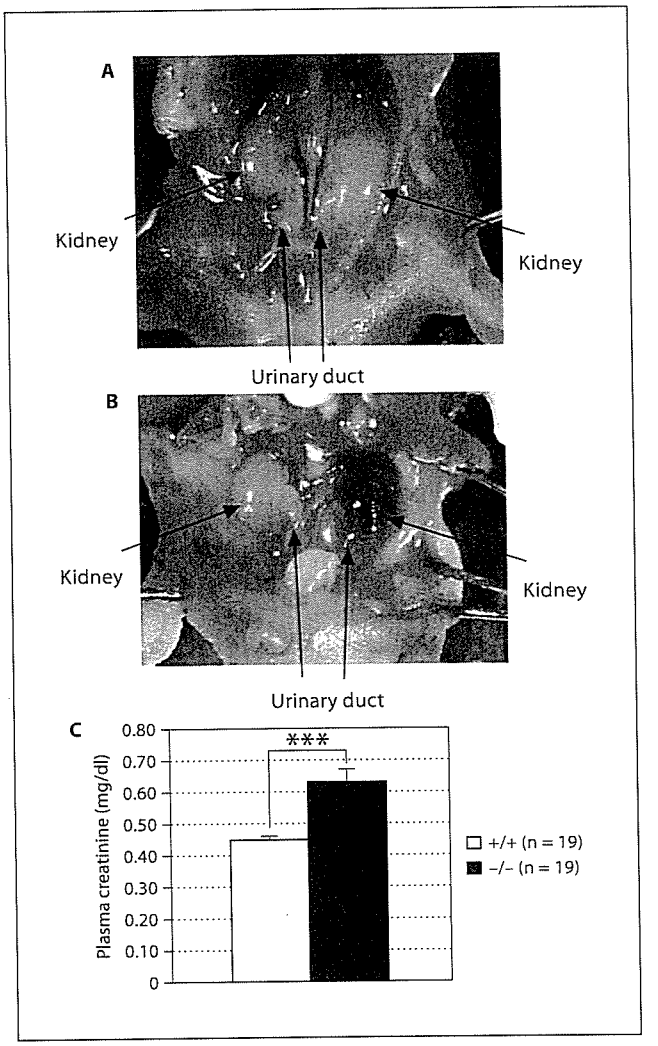

Fig. 5. Effects of *Lgr4* deficiency on the kidney of P0 mice. The morphology of the kidney and urinary duct in heterozygous (**A**) and null (**B**; no difference between wt and hetero mice; data not shown). The left kidney of the *Lgr4* null mouse shown was cystic. **C** To determine if the effects of *Lgr4* deficiency on the kidney were associated with functional changes, we measured plasma creatinine. *** $p < 0.001$, when compared with corresponding values from wt mice.

Fig. 6. Renal histopathology in the *Lgr4* null mice. Histology in a P0 wt mouse (**A**, **D**) and *Lgr4* null mice (**B**, **C**, **E–H**) is shown. Values on the left indicate the plasma creatinine concentration of each animal from which kidney and blood samples were prepared. **G**, **H** Unequally developed kidneys derived from a P0 null mouse. Each embedded kidney was sectioned at the region of maximum diameter. **A–C**, **G** Scale bar = 300 μm. **D–F**, **H** Scale bar = 60 μm.

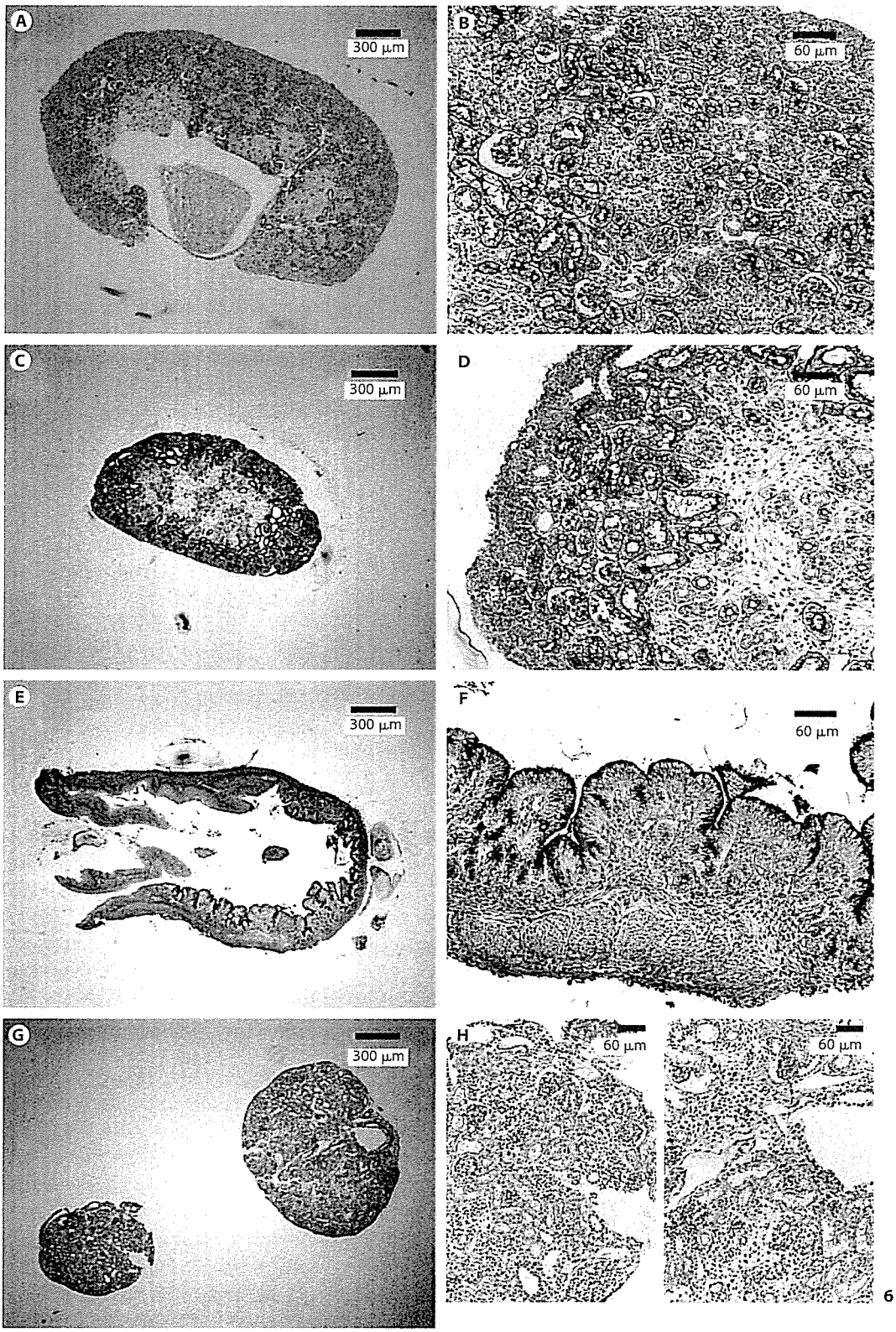
A
300 μm
B
60 μm
0.4
C
300 μm
D
60 μm
0.6
E
300 μm
F
60 μm
1.4
G
300 μm
H
60 μm
60 μm
0.8

6

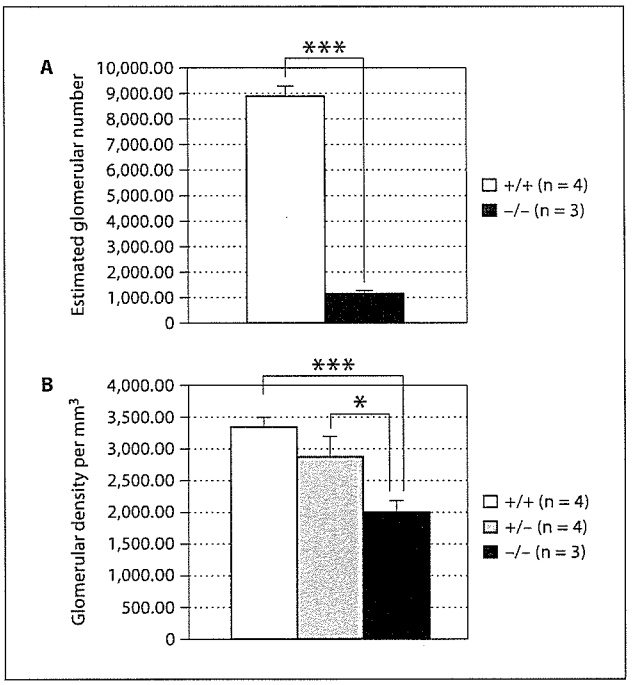

Fig. 7. Glomerular number (wild-type and *Lgr4* null) estimated and density (wt, *Lgr4* heterozygous and null) calculated in P0 mice. Mid slice sections were prepared, stained, and the numbers of glomeruli were counted. For an individual kidney, data from four non-adjacent sections (0.30 mm^2 apart; wt, heterozygous) or three non-adjacent sections (0.30 mm^2 apart; null) were obtained. Sections were prepared for 4 μm and wt kidney volume estimated 2.64 mm^3 and null estimated 0.58 mm^3. Data from 6 mice (wt and heterozygous) or 8 mice (null) were included. * $p < 0.05$ for null vs. heterozygous; *** $p < 0.001$ for null vs. wt.

later stages of kidney formation rather than to ureteric bud branching at early stages of nephron morphogenesis.

Discussion

In this report, we generated *Lgr4* gene-targeted mice with complete deletion of sequence encoding the LGR4 transmembrane and signal-transducing domains. Using the mutants, we demonstrate that *Lgr4* is required for normal kidney development and function to maintain filtration capacity without increasing the level of creatinine concentration. Null mice showed renal hypoplasia, and this phenotype was accompanied by functional failures as reflected in creatinine levels. Mazerbourg et al. [15] also recently reported the generation of a *Lgr4* knockout mouse model by gene trap methodology. They showed that deletion of *Lgr4* caused a phenotype most closely related to intrauterine growth retardation, to which they ascribed failure to thrive and perinatal lethality. However, abnormalities in individual organs possibly lead to perinatal lethality.

In contrast to the lower kidney weights in *Lgr4* gene trap mice seen by Mazerbourg et al. [15], the kidneys of null mice in our study are hypoplastic with a low density of glomeruli, leading to massive tissue damage in some cases, which indicates that *Lgr4* plays a critical role in kidney development. Despite kidney hypoplasia, however, a relatively normal glomerular structure was maintained until the accumulation of massive tissue damage. Although severe hypoplastic kidneys were observed in a few cases of *Lgr4* null mice, most of them showed merely a decreased kidney volume without structural defects. In contrast, 100% of *Lgr4* null mice showed an increased plasma creatinine concentration, perhaps reflecting an ensuing uremia contributing to perinatal death. Further experiments are required to discern whether the defect was simply caused by the decreased number of nephrons, or by a functional defect of the nephron unit in null mice.

Our findings suggest defects in the later stage of ureteric bud branching during nephrogenesis, although evagination of the ureteric bud and subsequent initial branching as well as differentiation of the metanephric mesenchyme have occurred normally in the null mice (fig. 8). Recent studies using knockout or transgenic mouse models have demonstrated the involvement of a number of key factors in determining nephron numbers, including fibroblast growth factor-10 [16, 17], *BMP-7* [18, 19] and so on. Although individual genes encoding these factors or receptors are expressed in various stages during nephrogenesis, they all share expression during branching morphogenesis. Kidneys of mice deficient in these genes showed histological phenotypes similar to the *Lgr4* null mice.

Although the ligand(s) and downstream effector(s) of LGR4 remain to be elucidated, the phenotype observed in the null mice allows us to speculate on the candidates. We expect that LGR4 will be involved with other molecules regulating the late stages of branching morphogenesis that determines nephron numbers. Mice with defects in GDNF-GFRα1-RET display renal hypoplasia [17, 20–22] similar to the LGR4 knockout phenotype. Profiling the gene expression in the null mice may also promote our understanding of the signaling pathway linked to

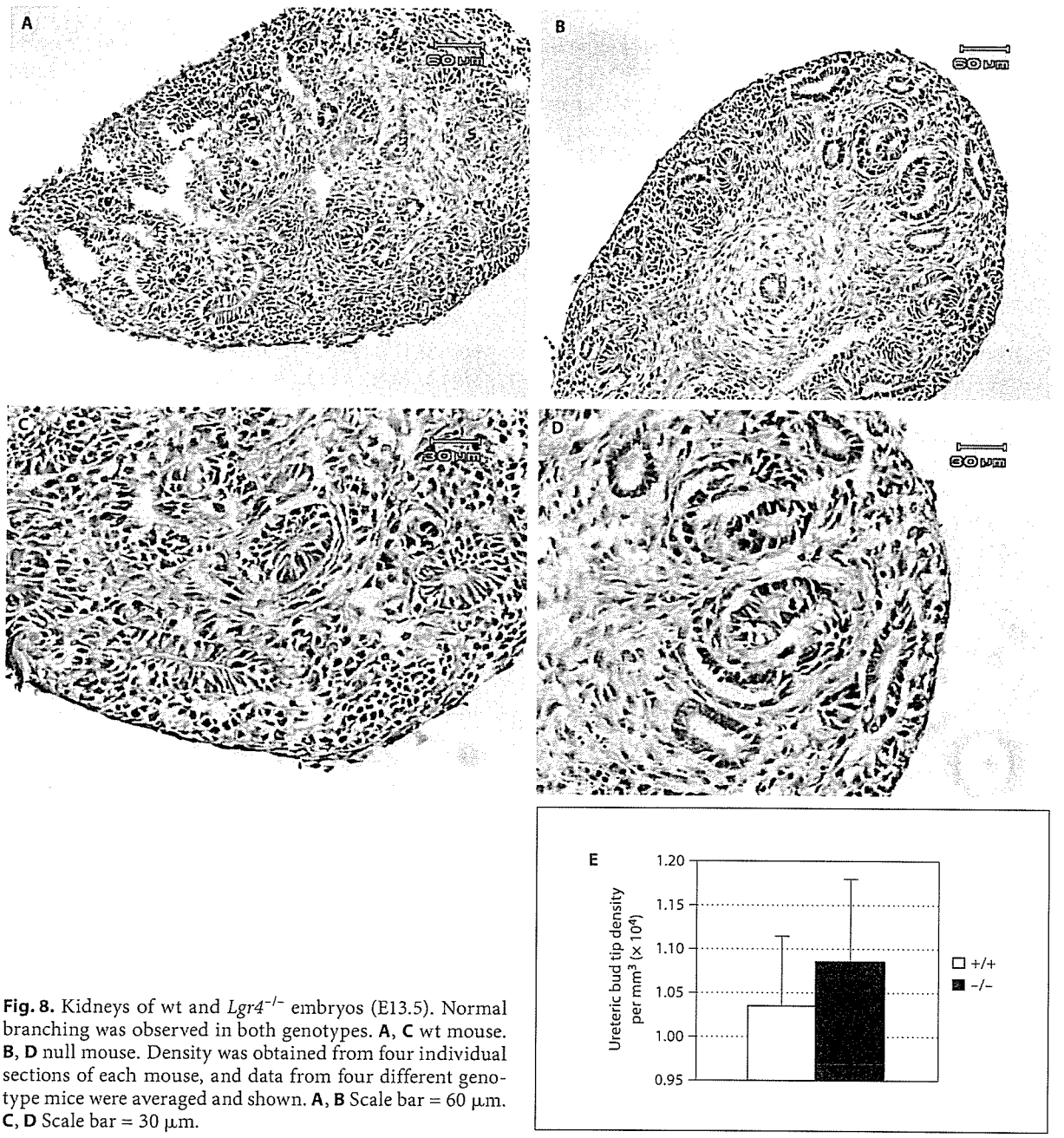

Fig. 8. Kidneys of wt and *Lgr4*$^{-/-}$ embryos (E13.5). Normal branching was observed in both genotypes. **A**, **C** wt mouse. **B**, **D** null mouse. Density was obtained from four individual sections of each mouse, and data from four different genotype mice were averaged and shown. **A**, **B** Scale bar = 60 μm. **C**, **D** Scale bar = 30 μm.

Lgr4. As some *Lgr4* null mice also display polycystic renal lesions, this suggests LGR4 might be involved in epithelial cellular polarity of other mechanisms that maintain renal tubule structure during nephrogenesis [23].

As compared to the study by Mazerbourg et al. [15], we observed greater penetrance of neonatal lethality and a more profound renal histopathological phenotype. The latter includes cystic lesions and a more subtle, perhaps precursor state of reduced nephron numbers and impaired renal function evident in mice surviving at birth (P0). These differences may be due to the different gene disruption strategies employed, or to genetic background

effects. Based on our findings we propose that renal dysfunction is a primary cause of the embryonic/neonatal lethality in *Lgr4* null mice.

In humans, the glomerular filtration rate is maintained in the face of renal insults, at first by the compensatory hyperfiltration of each glomerulus [24]. However beneficial in the short-term, prolongation of such overload causes glomerular sclerosis and renal failure in the long-term. Similarly, after uninephrectomy in young rats Nagata et al. [25] demonstrated that structural abnormalities in the glomeruli and a subsequent decrease in the glomerular filtration rate were never observed until 12 weeks after surgery. Some of the *Lgr4* null mice showed nephron agenesis with higher creatinine levels with first assessment at birth (P0; fig. 6C, F). In *Lgr4* null mice surviving to P2 and beyond, it is possible that gestational renal insults reach a critical state and manifest in renal failure early in postnatal life. Further experiments may be focused on assessing whether the severity of renal dysfunction in *Lgr4* null mice at birth and in the perinatal period is proportional to the extent of nephron number reduction as determined during nephrogenesis in utero.

While perinatal lethality was the predominant phenotype, one $Lgr4^{-/-}$ mouse survived longer. In histological analysis of its kidney upon necropsy, we observed dramatic cystic dilation of the renal tubules.

Other than the renal phenotype and intestinal dilation mentioned above, we also observed an the eyes open at birth phenotype in all of the *Lgr4* null mice. We have been studying the mechanism underlying this observation, and will report on this in the future.

In conclusion, we have generated a mouse model with complete deletion of *Lgr4* function and demonstrated that *Lgr4* is involved in nephrogenesis. We consider the lethality of *Lgr4* null mice as being closely related to renal dysfunction caused by impaired nephrogenesis. Circumventing the embryonic/neonatal lethal phenotype by a conditional knockout of *Lgr4* in mice will be useful for us to test this hypothesis and further study the functional role of *Lgr4* in individual tissues and organs.

Acknowledgments

We are grateful to Dr. T.R. Kumar (University of Kansas Medical Center) for his helpful discussions and critical review of the manuscript. We also thank Dr. N. Takamoto (Okayama University Medical School) for his valuable discussions and Dr. H. Suzuki for his encouragement. We thank Miss Y. Sato for providing the E14TG2a phage library. We also thank Dr. Y. Takayanagi for her excellent advice on manipulation of the mouse embryo. This work was supported in part by a grant-in-aid for scientific research (Hohga) from the Ministry of Education, Culture, Sports, Science and Technology of Japan (17659251) and by a grant from the Kureha Corporation.

References

▶1 Hsu SY, Liang SG, Hsueh AJ: Characterization of two LGR genes homologous to gonadotropin and thyrotropin receptors with extracellular leucine-rich repeats and a G protein-coupled, seven-transmembrane region. Mol Endocrinol 1998;12:1830–1845.

▶2 Heckert LL, Griswold MD: Expression of follicle-stimulating hormone receptor mRNA in rat testes and Sertoli cells. Mol Endocrinol 1991;5:670–677.

▶3 Sokka T, Hamalainen T, Huhtaniemi L: Functional LH receptor appears in the neonatal rat ovary after changes in the alternative splicing pattern of the LH receptor mRNA. Endocrinology 1992;130:1738–1740.

▶4 Hsu SY, Kudo M, Chen T, Nakabayashi K, Bhalla A, van der Spek PJ, van Duin M, Hsueh AJ: The three subfamilies of leucine-rich repeat-containing G protein-coupled receptors (LGR): identification of LGR6 and LGR7 and the signaling mechanism for LGR7. Mol Endocrinol 2000;14:1257–1271.

▶5 Krajnc-Franken MA, van Disseldorp AJ, Koenders JE, Mosselman S, van Duin M, Gossen JA: Impaired nipple development and parturition in LGR7 knockout mice. Mol Cell Biol 2004;24:687–696.

▶6 Kumagai J, Hsu SY, Matsumi H, Roh JS, Fu P, Wade JD, Bathgate RA, Hsueh AJ: INSL3/Leydig insulin-like peptide activates the LGR8 receptor important in testis descent. J Biol Chem 2002;277:31283–31286.

▶7 Kawamura K, Kumagai J, Sudo S, Chun SY, Pisarska M, Morita H, Toppari J, Fu P, Wade JD, Bathgate RA, Hsueh AJ: Paracrine regulation of mammalian oocyte maturation and male germ cell survival. Proc Natl Acad Sci USA 2004;101:7323–7328.

▶8 Hsu SY, Nakabayashi K, Nishi S, Kumagai J, Kudo M, Sherwood OD, Hsueh AJ: Activation of orphan receptors by the hormone relaxin. Science 2002;295:671–674.

▶9 Bullesbach EE, Schwabe C: LGR8 signal activation by the relaxin-like factor. J Biol Chem 2005;280:14586–14590.

▶10 Halls ML, Bathgate RA, Roche PJ, Summers RJ: Signaling pathways of the LGR7 and LGR8 receptors determined by reporter genes. Ann NY Acad Sci 2005;1041:292–295.

▶11 Matzuk MM, Finegold MJ, Su JG, Hsueh AJ, Bradley A: Alpha-inhibin is a tumour-suppressor gene with gonadal specificity in mice. Nature 1992;360:313–319.

▶12 Sakai K, Miyazaki J: A transgenic mouse line that retains Cre recombinase activity in mature oocytes irrespective of the cre transgene transmission. Biochem Biophys Res Commun 1997;237:318–324.

▶13 Nishimori K, Young LJ, Guo Q, Wang Z, Insel TR, Matzuk MM: Oxytocin is required for nursing but is not essential for parturition or reproductive behavior. Proc Natl Acad Sci USA 1996;93:11699–11704.

▶14 Duarte CG, Preuss HG: Assessment of renal function – glomerular and tubular. Clin Lab Med 1993;13:33–52.

▶15 Mazerbourg S, Bouley DM, Sudo S, Klein CA, Zhang JV, Kawamura K, Goodrich LV, Rayburn H, Tessier-Lavigne M, Hsueh AJ: Leucine-rich repeat-containing, G protein-coupled receptor 4 null mice exhibit intrauterine growth retardation associated with embryonic and perinatal lethality. Mol Endocrinol 2004;18:2241–2254.

▶16 Ohuchi H, Hori Y, Yamasaki M, Harada H, Sekine K, Kato S, Itoh N: FGF10 acts as a major ligand for FGF receptor 2 IIIb in mouse multi-organ development. Biochem Biophys Res Commun. 2000;277:643–649.

▶17 Qiao J, Bush KT, Steer DL, Stuart RO, Sakurai H, Wachsman W, Nigam SK: Multiple fibroblast growth factors support growth of the ureteric bud but have different effects on branching morphogenesis. Mech Dev 2001; 109:123–135.

▶18 Jena N, Martin-Seisdedos C, McCue P, Croce CM: BMP7 null mutation in mice: developmental defects in skeleton, kidney, and eye. Exp Cell Res 1997;230:28–37.

▶19 Dudley AT, Robertson EJ: Overlapping expression domains of bone morphogenetic protein family members potentially account for limited tissue defects in BMP7 deficient embryos. Dev Dyn 1997;208:349–362.

▶20 Sanchez MP, Silos-Santiago I, Frisen J, He B, Lira SA, Barbacid M: Renal agenesis and the absence of enteric neurons in mice lacking GDNF. Nature 1996;382:70–73.

▶21 Enomoto H, Araki T, Jackman A, Heuckeroth RO, Snider WD, Johnson EM Jr, Milbrandt J: GFR alpha1-deficient mice have deficits in the enteric nervous system and kidneys. Neuron 1998;21:317–324.

▶22 Jijiwa M, Fukuda T, Kawai K, Nakamura A, Kurokawa K, Murakumo Y, Ichihara M, Takahashi M: A targeting mutation of tyrosine 1062 in Ret causes a marked decrease of enteric neurons and renal hypoplasia. Mol Cell Biol 2004;24:8026–8036.

23 Wilson PD: Epithelial cell polarity and disease. Am J Physiol 1997;272:F434–F442.

24 Brenner BM, Garcia DL, S Anderson: Glomeruli and blood pressure. Less of one, more the other? Am J Hypertens 1998;1:335–347.

▶25 Nagata M, Scharer K, Kriz W: Glomerular damage after uninephrectomy in young rats. I. Hypertrophy and distortion of capillary architecture. Kidney Int 1992;42:136–147.

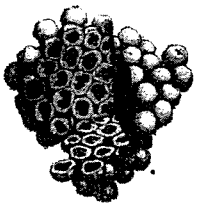

STEM CELLS®

A Comparison of Neural Differentiation and Retinal Transplantation with Bone Marrow-Derived Cells and Retinal Progenitor Cells

Minoru Tomita, Taisuke Mori, Kazuichi Maruyama, Tasneem Zahir, Matthew Ward, Akihiro Umezawa and Michael J. Young

Stem Cells 2006;24;2270-2278
DOI: 10.1634/stemcells.2005-0507

STEM CELLS®, an international peer-reviewed journal, covers all aspects of stem cell research: embryonic stem cells; tissue-specific stem cells; cancer stem cells; the stem cell niche; stem cell genetics and genomics; translational and clinical research; technology development.

STEM CELLS® is a monthly publication, it has been published continuously since 1983. The Journal is owned, published, and trademarked by AlphaMed Press, 318 Blackwell Street, Suite 260, Durham, North Carolina, 27701. Print ISSN: 1066-5099. Online ISSN: 1549-4918.

AlphaMed Press

STEM CELLS®
TISSUE-SPECIFIC STEM CELLS

A Comparison of Neural Differentiation and Retinal Transplantation with Bone Marrow-Derived Cells and Retinal Progenitor Cells

MINORU TOMITA,[a] TAISUKE MORI,[b,c] KAZUICHI MARUYAMA,[a] TASNEEM ZAHIR,[a] MATTHEW WARD,[a] AKIHIRO UMEZAWA,[b] MICHAEL J. YOUNG[a]

[a]The Schepens Eye Research Institute, Department of Ophthalmology, Harvard Medical School, Boston, Massachusetts, USA; [b]Department of Reproductive Biology and Pathology, National Research Institute for Child Health and Development, Tokyo, Japan; [c]Department of Pathology, Keio University, Tokyo, Japan

Key Words. Bone marrow stromal cells • Microglia • Retinal stem cells • Retinal transplantation • Neural differentiation

ABSTRACT

Retinal progenitor cells (RPCs) are immature precursors that can differentiate into retinal neurons, including photoreceptors. Recently, it has been reported that bone marrow-derived cells may also be capable of differentiation into cells of central nervous system lineage, including retinal neurons. We compared these two cell types to evaluate their potential as a source of cells for retinal transplantation. Marrow stromal cells (MSCs) and macrophages were isolated from enhanced green fluorescence protein mice. MSCs were cultured with brain-derived neurotrophic factor, nerve growth factor, and basic fibroblast growth factor to induce neuronal differentiation. RPCs were cultured under the same conditions or with 10% fetal bovine serum. Neuronal marker expression was examined and compared between MSCs and RPCs. MSCs, macrophages, and RPCs were also cultured with explanted retinas from rhodopsin knockout mice to study their potential for retinal integration. MSCs expressed neuronal and retina-specific markers by reverse transcription-polymerase chain reaction and immunocytochemistry. Both types of cells migrated into retinal explants and expressed neurofilament 200, glial fibrillary acidic protein, protein kinase C-α, and recoverin. RPCs expressed rhodopsin, a photoreceptor marker we never detected in MSCs. A majority of bone marrow derived-macrophages differentiated into cells that resembled microglia, rather than neural cells, in the explanted retina. This study shows that RPCs are likely to be a preferred cell type for retinal transplantation studies, compared with MSCs. However, MSCs may remain an attractive candidate for autologous transplantation. STEM CELLS *2006;24:2270–2278*

INTRODUCTION

Marrow stromal cells (MSCs) are a population of multipotent mesenchymal stem cells distinct from hematopoietic stem cells. MSCs were originally reported to contribute to the microenvironment of bone marrow and to be necessary for the proliferation of hematopoietic stem cells [1]. It has recently been shown that MSCs can differentiate into various cell lineages, including bone [2, 3], muscle [4], fat [5], cartilage [6], cardiomyocytes [7–9], and hepatocytes [10]. Recently, some studies claimed that MSCs could differentiate cells expressing markers of neurons and glia in vitro [11–17]. MSCs also have the capacity to migrate into the uninjured [18] and diseased brain [19, 20] and spinal cord [21, 22]. Interestingly, studies show that MSCs differentiate into cells expressing markers of photoreceptors and glia in the retina [23, 24].

The two major clinical subtypes of retinal degeneration (RD) are retinitis pigmentosa and age-related macular degeneration. A hallmark of these diseases is photoreceptor cell degeneration, resulting in visual loss. No effective restorative treatment exists for either RD subtype. Previously, we reported that brain-derived progenitor cells can migrate and differentiate into cells expressing markers of mature neurons and glia when grafted to the retina of mice and rats with RD [25–29]. Despite incorporation into the host retina and morphological similarities to various retinal cell types, the transplanted cells failed to express retina-specific markers in each of these studies. Recently, the transplantation of stem and progenitor cells isolated from retina has shown promise as a strategy for photoreceptor replacement [26, 28, 30–32]. Many mammalian tissues, including the retina, contain stem or progenitor cells that can be

Correspondence: Minoru Tomita, M.D., Ph.D., The Schepens Eye Research Institute, Department of Ophthalmology, Harvard Medical School, 20 Staniford St., Boston, Massachusetts 02114, USA. Telephone: 1-617-912-7419; Fax: 1-617-912-0101; e-mail: Minoru Tomita: tomita@vision.eri.harvard.edu; or Michael J. Young, Ph.D.: e-mail: mikey@vision.eri.harvard.edu Received October 12, 2005; accepted for publication May 23, 2006. © AlphaMed Press 1066-5099/2006/$20.00/0 doi: 10.1634/stemcells.2005-0507.

isolated, propagated, and grafted into animal models of RD [26, 32]. The goal of retinal transplantation is the replacement of dead or diseased host cells with healthy, functional donor cells. In the present study, we investigated whether MSCs could effectively differentiate into retinal cells by using a cocktail of brain-derived neurotrophic factor (BDNF), nerve growth factor (NGF), and basic fibroblast growth factor (bFGF), which (as we previously reported) induces MSC differentiation into neurons [17]. Because there are reports of the differentiation of microglial cells into neurons [33] and bone marrow-derived macrophages into brain microglia [34, 35], we examined the differentiation of macrophages when grafted into the retina. Here, we compared the potential of retinal progenitor cells (RPCs) and MSCs for use in retinal transplantation studies.

Materials and Methods

Experimental Animals

All experiments were performed in adherence with the ARVO (Association for Research in Vision and Ophthalmology) Statement for the Use of Animals in Ophthalmic and Vision Research and with the Schepens Eye Research Institute Animal Care and Use Committee (Boston, MA). Rhodopsin knockout mice (rho−/− mice; C57/Bl6 background, provided by Peter Humphries, University of Dublin, Trinity College, Dublin, Ireland) and postnatal day 1 (P1) enhanced green fluorescence protein (EGFP) mice (C57BL/6 background; Dr. Masaru Okabe, University of Osaka, Osaka, Japan) were euthanized by CO_2 gas.

Isolation of MSCs and Macrophages

Humeri, femurs, and tibias were obtained from P1 EGFP mice and divided into small pieces. These small pieces were cultured in Dulbecco's modified Eagle's medium (DMEM)/F-12 with 10% fetal bovine serum (FBS), and the nonadherent cells were removed by replacement of the media. After approximately 2 weeks, the adherent cells became confluent and were incubated with trypsin for 3 minutes and removed from the flask. All cell cultures were maintained at 37°C, 5% CO_2.

After two or three passages, bone marrow-derived adherent cells were incubated with trypsin for 3 minutes to generate a single-cell suspension. Cells (1×10^6) were labeled with phycoerythrin-conjugated antibody against CD11b (1:50, marker for macrophages; BD Biosciences PharMingen, San Diego, http://www.bdbiosciences.com) and Cy-5-conjugated antibody against CD45 (1:50, marker for hematopoietic cells; BD Biosciences PharMingen). To isolate MSCs ($CD45^-$, $CD11b^-$) and macrophages ($CD45^+$, $CD11b^+$) from bone marrow-derived adherent cells, cell sorting was performed (data not shown). After sorting, the isolated MSCs and macrophages were cultured in 20% FBS for 2–3 days and then used for the subsequent experiments.

RPC Line

RPCs harvested from the retina of P1 EGFP mice were isolated and maintained in culture as previously described [32]. Briefly, retinas were surgically removed. The tissue was finely minced with two scalpel blades (no. 10), these whole retina homogenates were incubated in 0.1% collagenase, and a single-cell suspension was obtained. Dissociated cells were then cultured in DMEM/F-12 supplemented with B27 (Invitrogen, Carlsbad, CA, http://www.invitrogen.com) and 20 ng/ml of epidermal growth factor (EGF). The neurospheres that were generated could in turn be dissociated and subcultured to generate new spheres [26, 32].

Neural Differentiation and Characterization of MSCs

To examine the differentiation of GFP-expressing MSCs in vitro, MSCs were incubated with trypsin for 3 minutes to generate a single-cell suspension. Cells (1×10^3) were plated on eight-well poly(D-lysine)/laminin-coated chamber slides (BD Biosciences, San Jose, CA, http://www.bdbiosciences.com) in DMEM/F-12 medium supplemented with 25 ng/ml BDNF (R&D Systems, Minneapolis, http://www.rndsystems.com), 40 ng/ml NGF (R&D Systems), and 20 ng/ml bFGF (R&D Systems) and were fixed with 4% paraformaldehyde (PFA) at 2 weeks after plating. The cells were blocked in 1% bovine serum albumin (Sigma-Aldrich, St. Louis, http://www.sigmaaldrich.com) + 0.2% Triton-100 (Sigma-Aldrich) and then incubated for 2 hours with primary antibody to Ki67 (1:100, cell proliferation marker; Vector Laboratories, Burlingame, CA, http://www.vectorlabs.com), nestin (1:1, immature neuronal marker; Developmental Studies Hybridoma Bank, Iowa City, IA, http://www.uiowa.edu/~dshbwww/), glial fibrillary acidic protein (GFAP) (1:50, astrocyte marker, Dako), MAP-2 (1:500, neuronal markers; Sigma-Aldrich), anti-protein kinase C (PKC)-α (1:200, bipolar cell marker; Santa Cruz Biotechnology, Inc., Santa Cruz, CA, http://www.scbt.com), 2D4 rhodopsin (1:500, rod photoreceptor marker; kind gift of Dr. R. Molday, University of British Columbia, Vancouver, BC, Canada), and recoverin antibodies (1:1,000, photoreceptor and bipolar cell marker; Chemicon International, Temecula, CA, http://www.chemicon.com). After rinsing in phosphate-buffered saline (PBS [0.1 M]), samples were incubated in Cy3-conjugated species-specific IgG (1:800) for 1 hour. Samples were rinsed again and then coverslipped in polyvinyl alcohol-1,4-diazabicyclo (2.2.2) octane (PVA-Dabco) with 4′,6-diamidino-2-phenylindole (DAPI) and viewed under fluorescent illumination. As a control, the untreated MSCs were fixed with 4% PFA and labeled with the same antibodies.

Differentiation and Characterization of RPCs

To examine the differentiation of GFP-expressing RPCs in vitro, RPC spheres were incubated with trypsin for 1 minute to generate a single-cell suspension. In two separate experiments, cells (1×10^3) were plated on eight-well poly(D-lysine)/laminin-coated chamber slides (BD Biosciences) in DMEM/F-12 medium supplemented either with 10% FBS or with BDNF, NGF, and bFGF (the same growth factors used in MSCs differentiation experiments [17]) and were then fixed with 4% PFA at 1 day and 2 weeks after plating. The cells were then reacted and prepared with the antibodies described for MSCs.

Morphometry of Differentiated Cells

In each of the three culture conditions (MSCs with BDNF, NGF, and bFGF; RPCs with 10% FBS; and RPCs with BDNF, NGF, and bFGF), quantitative morphometry was performed by counting positive cells from a total cell number of at least 200 cells per well in randomly selected wells, selected based on DAPI

labeling ($n = 5$). In this counting study, cells (1×10^3) were plated on eight-well poly(D-lysine)/laminin-coated chamber slides (BD Biosciences). Five of eight wells were randomly chosen (by a masked observer), and all cells in the wells were counted. Nestin-positive cells from RPCs were counted at day 1, and MSCs and RPCs positive for other markers were counted after 2 weeks of treatment.

Reverse Transcription-Polymerase Chain Reaction Analysis of MSCs

For reverse transcription-polymerase chain reaction (RT-PCR) analysis, total RNA was extracted using TRIzol (Invitrogen) from MSCs grown in the presence or absence of BDNF, NGF, and bFGF in poly(D-lysine)/laminin-coated culture dishes (BD Biosciences) and from P1 EGFP mice retina for a positive control. First-strand cDNA was prepared from total RNA by reverse transcriptase using oligo(dT) primers. To detect nestin, β-tubulin class III (BT-III; neuronal marker), Map2, GFAP, PKC-α, recoverin, and rhodopsin, primers were used as described in Table 1.

Retinal Organ Culture

Retinal organ culture was performed as previously described [36–38] with minor modifications. Briefly, eyes were enucleated from rhodopsin knockout (rho−/−) mice and transferred to ice-cold Hanks' balanced salt solution (Invitrogen). The retinas were separated from the retinal pigment epithelium and placed onto Millicell-CM membrane culture inserts (diameter 30 mm, pore size 0.4 μm; Millipore Corporation, Billerica, MA, http://www.millipore.com) with the ganglion cell layer downward. The inserts with neural retina were placed in six-well plates containing approximately 1 ml/well of medium containing DMEM/F-12 supplemented with B27 neural supplement (Invitrogen), 2 mM L-glutamine (Sigma-Aldrich), 2,000 U of nystatin (Invitrogen), and 100 μl/ml penicillin-streptomycin (Sigma-Aldrich). Organ cultures were maintained at 37°C, 5% CO_2 and fed every 2–3 days.

Explant Coculture

The host retinas were explanted from rho−/− mice (4–8 weeks of age). Cell suspensions (1 μl, 5×10^3 cells/μl) containing (a) RPCs ($n = 12$); (b) MSCs with ($n = 12$) or without ($n = 6$) pretreatment with BDNF, NGF, and bFGF for 1 week; and (c) macrophages ($n = 6$) were added to the retinas using a pipette immediately after isolation of recipient retinas. We placed the grafted cells onto the surface of retinal explants using a 200-μl pipette. The cells were spread out over the entire surface of the explant, confirmed by viewing under fluorescent illumination. The explanted retinas were cultured for 1 week.

Tissue Preparation

After 1 week in explant coculture, the explanted retinas were fixed with 4% PFA, followed by cryoprotection with 20% sucrose. The retinas were sectioned at 12 μm on a cryostat. Sections were stained with neurofilament (NF) 200 (1:1,000, neuronal marker; Sigma-Aldrich), GFAP, PKC-α, recoverin, and rhodopsin antibodies as described above. After fixation with PFA and sucrose, some whole-mount retinas were stained with biotin-*Griffonia simplicifolia* (GS)-lectin (5 μg/ml, microglia and macrophages marker; Sigma-Aldrich) for 15 minutes and NF200 antibody for 2 hours. After rinsing in PBS, samples were respectively incubated in Cy3-conjugated streptavidin (Jackson ImmunoResearch Laboratories, Inc., West Grove, PA, http://www.jacksonimmuno.com) and Cy3-conjugated species-specific IgG (1:800) for 1 hour. Samples were rinsed again and then coverslipped in PVA-Dabco and viewed under fluorescent illumination.

RESULTS

Characterization of MSCs

When grown on conventional substrates in media supplemented with 10% FBS, GFP-transgenic MSCs exhibited high levels of endogenous green fluorescence (Fig. 1A). The untreated MSCs did not express nestin, Map2, GFAP, PKC-α, recoverin, or rhodopsin (data not shown). To examine differentiation in vitro, medium without 10% FBS was supplemented with BDNF, NGF, and bFGF. After 2 weeks of culture under differentiation conditions, MSCs differentiated into cells with neuronal morphologies and neurite-like processes (Fig. 1B) and also formed spheres (Fig. 1C). Subpopulations of MSCs expressed nestin (Fig. 1D–1F), Map2 (Fig. 1G–1I), GFAP (Fig. 1J–1L), PKC-α (Fig. 1M–1O), and recoverin (Fig. 1P–1R). These markers are consistent, although not conclusive, with differentiation into

Table 1. Primers used for reverse transcription-polymerase chain reaction analysis

Genes	Primer sequences (5′–3′)	Product size (bp)	Temperature (°C)
Nestin	F: AACTGGCACACCTCAAGATGT R: TCAAGGGTATTAGGCAAGGGG	235	60
GFAP	F: CACGAACGAGTCCCTAGAGC R: ATGGTGATGCGGTTTTCTTC	234	60
TB-III	F: ACCTCAACCACCTGGTATCG R: TGCTGTTCTTGCTCTGGATG	344	60
Map2	F: CTGGACATCAGCCTCACTCA R:AATAGGTGCCCTGTGACCTG	164	60
PKC-α	F: CCCATTCCAGAAGGAGATGA R: TTCCTGTCAGCAAGCATCAC	212	60
Recoverin	F: ATGGGGAATAGCAAGAGCGG R: GAGTCCGGGAAAAACTTGGAATA	179	60
Rhodopsin	F: TCACCACCACCCTCTACACA R: TGATCCAGGTGAAGACCACA	216	60

Abbreviations: bp, base pair; F, forward; GFAP, glial fibrillary acidic protein; PKC, protein kinase C; R, reverse; TB, tubulin.

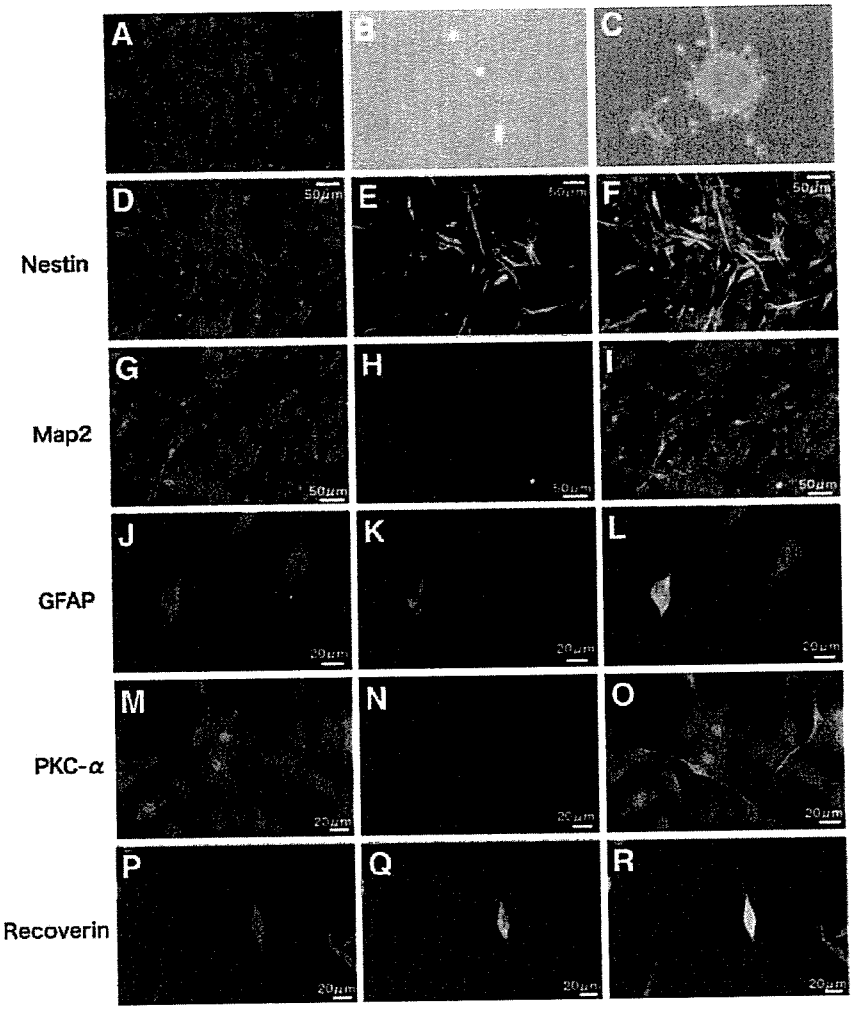

Figure 1. Differentiation and characterization of marrow stromal cell (MSCs) in vitro. Undifferentiated GFP$^+$ MSCs grown in Dulbecco's modified Eagle's medium with 10% fetal bovine serum, viewed under fluorescein isothiocyanate illumination (**A**). MSCs cultured in serum-free medium with brain-derived neurotrophic factor, nerve growth factor, and basic fibroblast growth factor for 14 days (**B–R**). After 2 weeks of culture under differentiation conditions, MSCs morphologically differentiated into neuronal shape and had neuronal processes (**B**) and also formed spheres (**C**). Constitutive GFP expression (**D, G, J, M, P**), antibody/cytokeratin-3 immunoreactivity for nestin (**E**), Map2 (**H**), GFAP (**K**), PKC-α (**N**), and recoverin (**Q**), and merged images (**F, I, L, O, R**). Abbreviations: GFAP, glial fibrillary acidic protein; GFP, green fluorescent protein; PKC, protein kinase C.

retinal neurons. Interestingly, these immunopositive cells also showed morphological evidence suggestive of differentiation into immature photoreceptors, bipolar cell types, glial cells, and neuronal cells (Fig. 1F, 1I, 1L, 1O, 1R). We could not find any rhodopsin-positive cells from treated MSCs.

Characterization of RPCs

When grown on conventional substrates in medium supplemented with EGF, GFP-transgenic RPCs exhibited high levels of endogenous green fluorescence (Fig. 2A) and maintained an undifferentiated state characterized by ubiquitous Ki67 and nestin immunoreactivity (Fig. 2B, 2C). Cells could be maintained in this state for up to 1 year or 50 passages as neurospheres. To examine differentiation in vitro, medium without EGF was supplemented with 10% FBS. After 2 weeks culture under differentiation conditions, the cells were analyzed immunocytochemically. The number of Ki67$^+$ cells markedly decreased (data not shown), and subpopulations expressed GFAP (Fig. 2D), Map2 (Fig. 2E), PKC-α (Fig. 2F), recoverin (Fig. 2G), or rhodopsin (Fig. 2H). These markers are consistent with differentiation into rod photoreceptors, bipolar cells, and Muller glia, all of which are known to be born late in retinogenesis. Moreover, these immunopositive cells also showed morphological evidence suggestive of immature photoreceptor differentiation, as well as of other retinal cell types (Fig. 2D–2H).

Quantitative Evaluation of Differentiated Cell Numbers: MSCs Versus RPCs

To examine the optimal source of cells for retinal transplantation, quantitative evaluation of differentiation into neuronal and retinal cells was carried out using cell counting as previously described [39].

After 2 weeks of BDNF, NGF, and bFGF treatment, the percentages of surviving MSCs expressing nestin, Map2, GFAP, PKC-α, and recoverin were 5.55%, 3.27%, 1.42%, 3.97%, and 13.9%, respectively. The percentages of nestin-, Map2-, GFAP-, PKC-α-, recoverin-, and rhodopsin-positive cells from RPCs treated with 10% FBS were 90.5%, 15.2%, 64.4%, 12.9%, 23.6%, and 3.17%, respectively. The rates of nestin-, Map2-, GFAP-, PKC-α-, recoverin-, and rhodopsin-positive cells from RPCs treated with BDNF, NGF, and bFGF were 89.2%, 29.4%, 10.9%, 28.2%, 22.3%, and 2.25%, respectively (Fig. 3A).

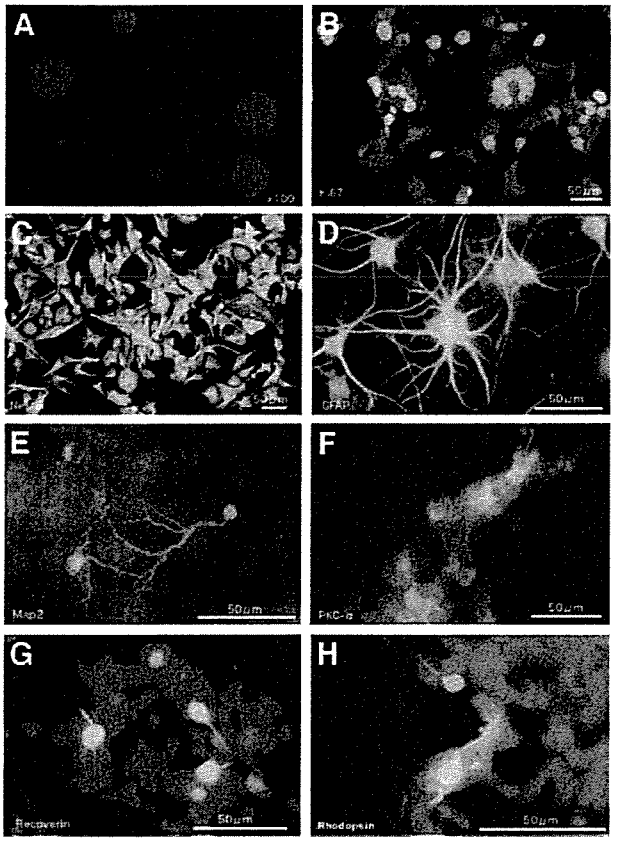

Figure 2. Differentiation and characterization of retinal progenitor cell (RPCs) in vitro. RPCs formed green fluorescent protein-positive neurospheres (**A**). RPCs cultured in the absence of epidermal growth factor and in the presence of 10% fetal bovine serum for 1 (**B, C**) or 14 (**D–H**) days. The cells were stained for Ki67 (**B**), nestin (**C**), GFAP (**D**), Map2 (**E**), PKC-α (**F**), recoverin (**G**), and rhodopsin (**H**). Abbreviations: GFAP, glial fibrillary acidic protein; MSC, marrow stromal cell; PKC, protein kinase C.

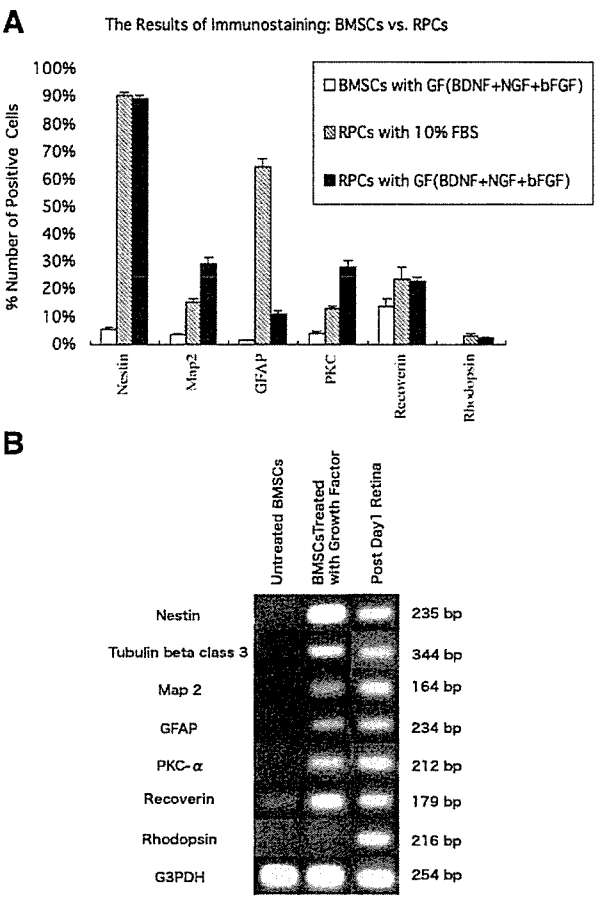

Figure 3. Comparison of BMSCs and RPCs. (**A**): The number of cells differentiated into retinal cells: comparison of marrow stromal cell (MSCs) and RPCs. In this study, nestin-positive cells were counted at day 1, and other markers cells were counted at 2 weeks after treatment. (**B**): Effect of BDNF, NGF, and bFGF on transcription of retinal cell markers. Semiquantitative reverse transcription-polymerase chain reaction analysis was carried out to determine the effect of BDNF, NGF, and bFGF on MSCs. MSCs without treatment showed only weak recoverin expression. (MSCs without treatment did not express nestin, BT-III, Map2, GFAP, PKC-α, and rhodopsin completely.) After 2 weeks of BDNF, NGF, and bFGF treatment, treated MSCs expressed nestin, BT-III, Map2, GFAP, PKC-α, and recoverin; however, rhodopsin expression was not found. Recoverin expression was increased in treated MSCs. Abbreviations: BDNF, brain-derived neurotrophic factor; bFGF, basic fibroblast growth factor; BMSC, bone marrow stromal cell; bp, base pair; BT-III, β-tubulin class III; FBS, fetal bovine serum; GF, growth factor; GFAP, glial fibrillary acidic protein; NGF, nerve growth factor; PKC, protein kinase C; RPC, retinal progenitor cell.

RT-PCR Analysis of BDNF, NGF, and bFGF Treatment

Semiquantitative RT-PCR analysis was carried out to determine the effect of BDNF, NGF, and bFGF on MSCs (Fig. 3B). MSCs without treatment showed only weak recoverin expression. (MSCs without treatment did not express nestin, BT-III, Map2, GFAP, PKC-α, or rhodopsin.) After 2 weeks of BDNF, NGF, and bFGF treatment, MSCs expressed nestin, BT-III, Map2, GFAP, PKC-α, and recoverin. Rhodopsin expression was not found. Recoverin expression was increased in treated MSCs.

Macrophages Differentiated into Microglia After Coculture with Explanted Retinas

After coculture with explanted rho−/− mouse retinas, macrophages were viewed by fluorescent illumination at 3 and 7 days. Macrophages migrated into the retina and assumed morphology very reminiscent of microglial cells (Fig. 4A–4C). The cocultured macrophages also expressed GS-lectin, a marker of microglia (Fig. 4D–4F). There was no evidence of neuronal differentiation upon immunocytochemical and morphological analyses (data not shown).

Migration and Differentiation of MSCs

At 1 week in coculture, MSCs with and without pretreatment of BDNF, NGF, and bFGF migrated into explanted rho−/− retina (Fig. 5A). MSCs without pretreatment did not show morphological or immunocytochemical evidence of neural differentiation (data not shown). On the other hand, pretreated MSCs showed morphological and immunocytochemical evidence of neuronal differentiation. Pretreated MSCs migrated into explanted retinas (Fig. 5A) and expressed NF200 (Fig. 5B–5G), GFAP (Fig. 5H–5J), PKC-α (Fig. 5K–5M), and recoverin (Fig.

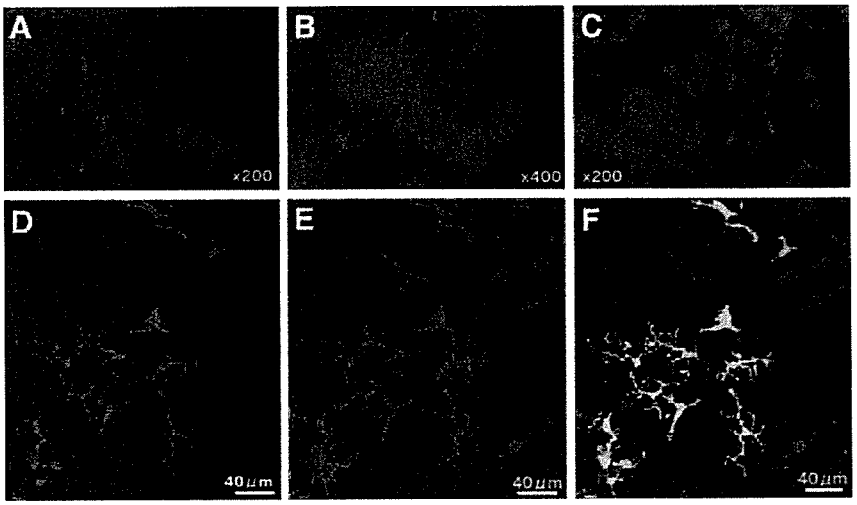

Figure 4. Macrophages differentiated into microglia after transplantation to explanted retinas. Rho−/− mice retina at 3 (**A**) and 7 (**B, C**) days. Macrophages migrated into retina and morphologically changed their shape to that resembling microglia (**A–C**). Confocal (**D–F**) images seen at 1 week after grafting; constitutive green fluorescent protein expression (**D**), macrophage/microglia antibody/cytokeratin-3 immunoreactivity (**E**), and merged images (**F**).

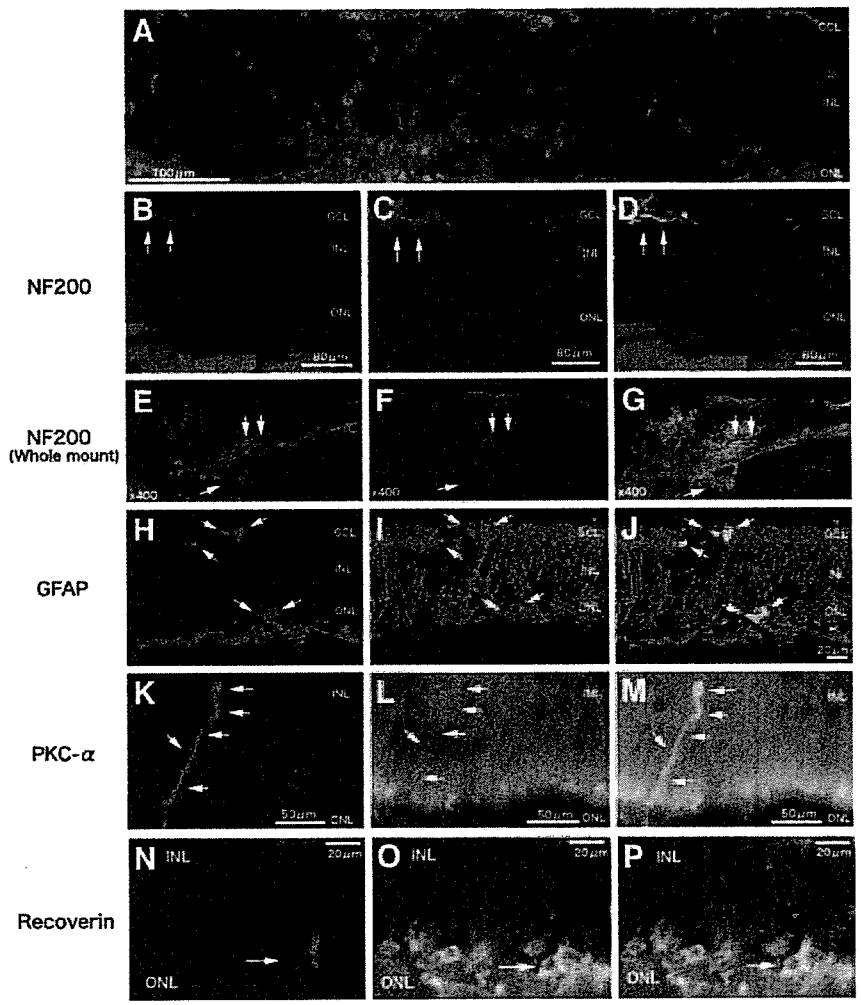

Figure 5. Migration and differentiation of pretreated marrow stromal cell (MSCs) into explanted retinas of rho−/− mice. A large number of MSCs migrated into explanted retinas of rho−/− mice (**A**). Epi-fluorescent (**K–P**) and confocal (**B–J**) images of the expression of neural and photoreceptor markers by pretreated MSCs that were grafted onto explanted retinas from rho−/− mice, seen at 1 week after grafting; constitutive green fluorescent protein expression (**B, E, H, K, N**), antibody/cytokeratin-3 immunoreactivity for NF200 (**C, F**) (whole mount), GFAP (**I**), PKC-α (**L**), recoverin (**O**), and merged images (**D, G, J, M, P**). Abbreviations: GCL, ganglion cell layer; GFAP, glial fibrillary acidic protein; INL, inner nuclear layer; NF, neurofilament; ONL, outer nuclear layer; PKC, protein kinase C.

5N–5P). We also found morphological evidence of neuronal differentiation (Fig. 5B–5P). However, we could not find any rhodopsin-positive cells among coculture, pretreated MSCs.

Migration and Differentiation of RPCs

At 1 week in coculture, RPCs migrated into all retinal lamina adjacent to the graft after addition to the outer retina and showed

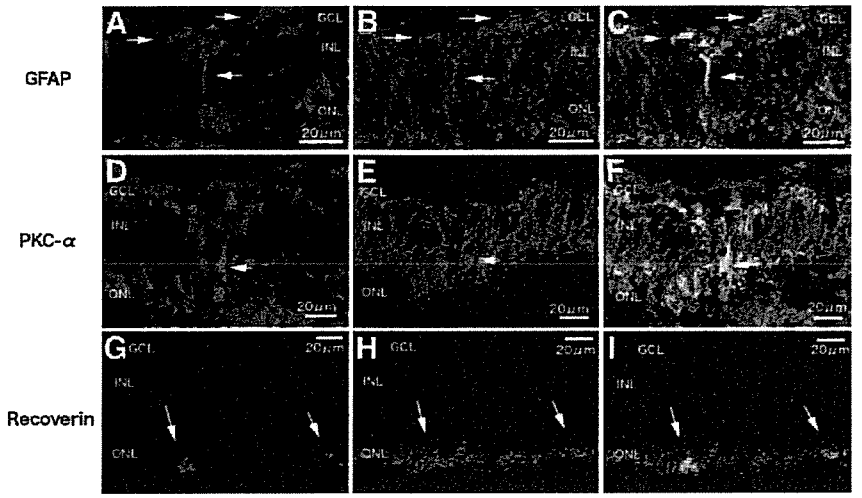

Figure 6. Migration and differentiation of pretreated retinal progenitor cells (RPCs) into explanted retinas of rho−/− mice. Confocal images of the expression of neural and photoreceptor markers by RPCs grafting to explanted retinas of rho−/− mice, seen at 1 week after grafting; constitutive green fluorescent protein expression (**A, D, G**), antibody/cytokeratin-3 immunoreactivity for GFAP (**B**), PKC-α (**E**), recoverin (**H**), and merged images (**C, F, I**). Abbreviations: GCL, ganglion cell layer; GFAP, glial fibrillary acidic protein; INL, inner nuclear layer; MSC, marrow stromal cell; ONL, outer nuclear layer; PKC, protein kinase C.

morphological evidence of neuronal differentiation (Fig. 6D–6I). GFP^+ donor cells coexpressed a number of markers indicative of phenotypic maturation, including GFAP (Fig. 6A–6C), PKC-α (Fig. 6D–6F), and recoverin (Fig. 6G–6I). In the rho−/− mice, the rod marker rhodopsin was not detected in either grafted RPCs or the host outer nuclear layer.

Discussion

The results presented here demonstrate that MSCs treated with BDNF, NGF, and bFGF can differentiate into retinal cells expressing Map2, BT-III, GFAP, PKC-α, and recoverin by immunocytochemistry and RT-PCR. In the explanted retina, pretreated MSCs showed differentiation into retinal cells expressing NF200, GFAP, PKC-α, and recoverin, although nonpretreated MSCs did not show any evidence of differentiation into retinal cells. This shows that treatment with growth factors (as in our previous report [17]) is very important for neural induction of MSCs. Moreover, our data show that using growth factors promoted neuronal differentiation over glial differentiation in RPCs (Fig. 3A). In the present study, RPCs clearly showed a higher level of differentiation into retinal cells compared with MSCs. Induced MSCs expressed neuronal and glial markers and morphologically differentiated into neuron- and glia-like cells; however, RPCs showed better morphological differentiation and also expressed rhodopsin (Figs. 1, 2). Although a subpopulation of MSCs differentiated morphologically into neuronal-like cells and expressed neuronal markers, the majority remained undifferentiated both in terms of morphology and marker expression during the time course examined. The lack of rhodopsin expression in vivo and in vitro by MSCs may be an impediment to their use in photoreceptor replacement. One must be cognizant of the fact that the absence of evidence is not evidence of absence. The lack of differentiation in vitro indicates that the optimal conditions have yet to be determined. This is especially true in the case of RPC photoreceptor differentiation, which we have shown to be dependent upon specific conditions in vivo. The fact that RPCs failed to express rhodopsin after migration into explants is not surprising, considering that our previous studies found no evidence for rhodopsin among RPCs transplanted to rho−/− mice in vivo [32]. The same study showed that RPCs expressed rhodopsin in another mouse strain with RD, the C3H mouse [32].

As with previous studies in the brain [34, 35], our results showed that macrophages migrated into explanted retina and appeared to differentiate into microglia. Although a previous report showed that microglia have potential for neuronal differentiation [33], we did not find evidence of differentiation into neuronal or glial cells in our explant study. Further studies will be needed to determine the neuronal potential of macrophages and microglia.

From a clinical perspective, MSCs are a good source for stem cell transplantation. Bone marrow cell transplantation is already an approved therapy for some kinds of hematological diseases and has the advantage of the possibility of autologous cell transplantation. Moreover, because recent reports have shown that MSCs have the capacity to modulate allogeneic cellular immunity [40, 41], MSCs may be useful for allogeneic transplantation.

Cell fusion has recently been proposed as the underlying explanation for the apparent plasticity and "transdifferentiation" of stem cells, including MSCs. This raises questions about the mechanisms of transdifferentiation in vitro and in vivo [42, 43]. Evidence against cell fusion has begun to mount; recent studies reported that MSCs can undergo transdifferentiation into various organ cell types, including neurons, without fusion [10, 44, 45]. We believe that our results cannot be attributed to cell fusion; this study shows that MSC differentiation into post-mitotic neuronal and retinal cells occurred in a controlled culture environment. Recent studies have shown that MSCs have a potential of transdifferentiation as cultured MSCs express mesodermal, endodermal, ectodermal, and germline genes, suggesting the potential to differentiate into all these cell types [46–48]. Moreover, our previous study [17], using the same methods for neuronal induction as this study, showed neuroectodermal induction, neural differentiation, and calcium uptake in response to a depolarizing stimulus from human MSCs. It has also been reported that neuroectodermal induction and electrophysiological characteristics of midbrain dopaminergic, serotonergic, and GABA-ergic neurons arise from treated MSCs [16].

CONCLUSION

The present study shows that RPCs have clear advantages over MSCs in potential retinal transplantation applications. First, no evidence was found for MSC differentiation into rod photoreceptors. Second, RPCs showed more complete differentiation into retinal cell subtypes than did MSCs, and this occurred at a significantly higher rate. Finally, we have previously reported that neuronal progenitor cells (NPCs) have inherent immune privilege, suggesting increased resistance of allogeneic NPC grafts to host rejection [49, 50]. Such findings suggest the possibility that RPCs possess immune privilege properties as well. MSCs also have significant therapeutic potential in transplantation medicine because they can be readily obtained through a well-established clinical procedure. They are relatively easy to isolate and expand for autologous transplantation without the need for immunosuppression or the risk of rejection. In this comparison study, we submit that RPCs possess significant advantages for differentiation into retinal cells compared with MSCs.

ACKNOWLEDGMENTS

This work was supported by grants from the U.S. Department of Defense, National Institutes of Health (09595; M.J.Y.), and by a gift from Richard and Gail Siegal. We thank Prof. Susumu Ikehara (Department of Pathology, Kansai Medical University, Osaka, Japan) for advice.

DISCLOSURES

The authors indicate no potential conflicts of interest.

REFERENCES

1 Dexter TM, Allen TD, Lajtha LG. Conditions controlling the proliferation of haemopoietic stem cells in vitro. J Cell Physiol 1977;91:335–344.

2 Rickard DJ, Sullivan TA, Shenker BJ et al. Induction of rapid osteoblast differentiation in rat bone marrow stromal cell cultures by dexamethasone and BMP-2. Dev Biol 1994;161:218–228.

3 Tsuchiya K, Mori T, Chen G et al. Custom-shaping system for bone regeneration by seeding marrow stromal cells onto a web-like biodegradable hybrid sheet. Cell Tissue Res 2004;316:141–153.

4 Ferrari G, Cusella-De Angelis G, Coletta M et al. Muscle regeneration by bone marrow-derived myogenic progenitors. Science 1998;279: 1528–1530.

5 Umezawa A, Tachibana K, Harigaya K et al. Colony-stimulating factor 1 expression is down-regulated during the adipocyte differentiation of H-1/A marrow stromal cells and induced by cachectin/tumor necrosis factor. Mol Cell Biol 1991;11:920–927.

6 Ashton BA, Allen TD, Howlett CR et al. Formation of bone and cartilage by marrow stromal cells in diffusion chambers in vivo. Clin Orthop Relat Res 1980;151:294–307.

7 Orlic D, Kajstura J, Chimenti S et al. Bone marrow cells regenerate infarcted myocardium. Nature 2001;410:701–705.

8 Takeda Y, Mori T, Imabayashi H et al. Can the life span of human marrow stromal cells be prolonged by bmi-1, E6, E7, and/or telomerase without affecting cardiomyogenic differentiation? J Gene Med 2004;6: 833–845.

9 Makino S, Fukuda K, Miyoshi S et al. Cardiomyocytes can be generated from marrow stromal cells in vitro. J Clin Invest 1999;103:697–705.

10 Sato Y, Araki H, Kato J et al. Human mesenchymal stem cells xenografted directly to rat liver differentiated into human hepatocytes without fusion. Blood 2005;106:756–763.

11 Woodbury D, Schwarz EJ, Prockop DJ et al. Adult rat and human bone marrow stromal cells differentiate into neurons. J Neurosci Res 2000; 61:364–370.

12 Kohyama J, Abe H, Shimazaki T et al. Brain from bone: Efficient "meta-differentiation" of marrow stroma-derived mature osteoblasts to neurons with Noggin or a demethylating agent. Differentiation 2001;68: 235–244.

13 Suzuki H, Taguchi T, Tanaka H et al. Neurospheres induced from bone marrow stromal cells are multipotent for differentiation into neuron, astrocyte, and oligodendrocyte phenotypes. Biochem Biophys Res Commun 2004;322:918–922.

14 Sanchez-Ramos J, Song S, Cardozo-Pelaez F et al. Adult bone marrow stromal cells differentiate into neural cells in vitro. Exp Neurol 2000; 164:247–256.

15 Neuhuber B, Gallo G, Howard L et al. Reevaluation of in vitro differentiation protocols for bone marrow stromal cells: Disruption of actin cytoskeleton induces rapid morphological changes and mimics neuronal phenotype. J Neurosci Res 2004;77:192–204.

16 Jiang Y, Henderson D, Blackstad M et al. Neuroectodermal differentiation from mouse multipotent adult progenitor cells. Proc Natl Acad Sci U S A 2003;100:11854–11860.

17 Mori T, Kiyono T, Imabayashi H et al. Combination of hTERT and bmi-1, E6, or E7 induces prolongation of the life span of bone marrow stromal cells from an elderly donor without affecting their neurogenic potential. Mol Cell Biol 2005;25:5183–5195.

18 Kopen GC, Prockop DJ, Phinney DG. Marrow stromal cells migrate throughout forebrain and cerebellum, and they differentiate into astrocytes after injection into neonatal mouse brains. Proc Natl Acad Sci U S A 1999;96:10711–10716.

19 Chopp M, Li Y. Treatment of neural injury with marrow stromal cells. Lancet Neurol 2002;1:92–100.

20 Dezawa M, Kanno H, Hoshino M et al. Specific induction of neuronal cells from bone marrow stromal cells and application for autologous transplantation. J Clin Invest 2004;113:1701–1710.

21 Akiyama Y, Radtke C, Honmou O et al. Remyelination of the spinal cord following intravenous delivery of bone marrow cells. Glia 2002; 39:229–236.

22 Hofstetter CP, Schwarz EJ, Hess D et al. Marrow stromal cells form guiding strands in the injured spinal cord and promote recovery. Proc Natl Acad Sci U S A 2002;99:2199–2204.

23 Tomita M, Adachi Y, Yamada H et al. Bone marrow-derived stem cells can differentiate into retinal cells in injured rat retina. STEM CELLS 2002;20:279–283.

24 Kicic A, Shen WY, Wilson AS et al. Differentiation of marrow stromal cells into photoreceptors in the rat eye. J Neurosci 2003;23:7742–7749.

25 Mizumoto H, Mizumoto K, Shatos MA et al. Retinal transplantation of neural progenitor cells derived from the brain of GFP transgenic mice. Vision Res 2003;43:1699–1708.

26 Klassen H, Sakaguchi DS, Young MJ. Stem cells and retinal repair. Prog Retin Eye Res 2004;23:149–181.

27 Young MJ, Ray J, Whiteley SJ et al. Neuronal differentiation and morphological integration of hippocampal progenitor cells transplanted to the retina of immature and mature dystrophic rats. Mol Cell Neurosci 2000;16:197–205.

28 Klassen H, Ziaeian B, Kirov II et al. Isolation of retinal progenitor cells from post-mortem human tissue and comparison with autologous brain progenitors. J Neurosci Res 2004;77:334–343.

29 Lu B, Kwan T, Kurimoto Y et al. Transplantation of EGF-responsive neurospheres from GFP transgenic mice into the eyes of rd mice. Brain Res 2002;943:292–300.

30 Ahmad I, Dooley CM, Thoreson WB et al. In vitro analysis of a mammalian retinal progenitor that gives rise to neurons and glia. Brain Res 1999;831:1–10.

31 Tropepe V, Coles BL, Chiasson BJ et al. Retinal stem cells in the adult mammalian eye. Science 2000;287:2032–2036.

32 Klassen HJ, Ng TF, Kurimoto Y et al. Multipotent retinal progenitors express developmental markers, differentiate into retinal neurons, and preserve light-mediated behavior. Invest Ophthalmol Vis Sci 2004;45: 4167–4173.

33 Yokoyama A, Yang L, Itoh S et al. Microglia, a potential source of neurons, astrocytes, and oligodendrocytes. Glia 2004;45:96–104.

34 Tanaka R, Komine-Kobayashi M, Mochizuki H et al. Migration of enhanced green fluorescent protein expressing bone marrow-derived microglia/macrophage into the mouse brain following permanent focal ischemia. Neuroscience 2003;117:531–539.

35 Eglitis MA, Mezey E. Hematopoietic cells differentiate into both microglia and macroglia in the brains of adult mice. Proc Natl Acad Sci U S A 1997;94:4080–4085.

36 Zhang Y, Caffe AR, Azadi S et al. Neuronal integration in an abutting-retinas culture system. Invest Ophthalmol Vis Sci 2003;44:4936–4946.

37 Zhang Y, Kardaszewska AK, van Veen T et al. Integration between abutting retinas: Role of glial structures and associated molecules at the interface. Invest Ophthalmol Vis Sci 2004;45:4440–4449.

38 Akita J, Takahashi M, Hojo M et al. Neuronal differentiation of adult rat hippocampus-derived neural stem cells transplanted into embryonic rat explanted retinas with retinoic acid pretreatment. Brain Res 2002;954: 286–293.

39 Zahir T, Klassen H, Young MJ. Effects of ciliary neurotrophic factor on differentiation of late retinal progenitor cells. STEM CELLS 2005;23: 424–432.

40 Aggarwal S, Pittenger MF. Human mesenchymal stem cells modulate allogeneic immune cell responses. Blood 2005;105:1815–1822.

41 Beyth S, Borovsky Z, Mevorach D et al. Human mesenchymal stem cells alter antigen-presenting cell maturation and induce T-cell unresponsiveness. Blood 2005;105:2214–2219.

42 Alvarez-Dolado M, Pardal R, Garcia-Verdugo JM et al. Fusion of bone-marrow-derived cells with Purkinje neurons, cardiomyocytes and hepatocytes. Nature 2003;425:968–973.

43 Weimann JM, Johansson CB, Trejo A et al. Stable reprogrammed heterokaryons form spontaneously in Purkinje neurons after bone marrow transplant. Nat Cell Biol 2003;5:959–966.

44 Pochampally RR, Neville BT, Schwarz EJ et al. Rat adult stem cells (marrow stromal cells) engraft and differentiate in chick embryos without evidence of cell fusion. Proc Natl Acad Sci U S A 2004;101:9282–9285.

45 Cogle CR, Yachnis AT, Laywell ED et al. Bone marrow transdifferentiation in brain after transplantation: A retrospective study. Lancet 2004; 363:1432–1437.

46 Tremain N, Korkko J, Ibberson D et al. MicroSAGE analysis of 2,353 expressed genes in a single cell-derived colony of undifferentiated human mesenchymal stem cells reveals mRNAs of multiple cell lineages. STEM CELLS 2001;19:408–418.

47 Seshi B, Kumar S, King D. Multilineage gene expression in human bone marrow stromal cells as evidenced by single-cell microarray analysis. Blood Cells Mol Dis 2003;31:268–285.

48 Woodbury D, Reynolds K, Black IB. Adult bone marrow stromal stem cells express germline, ectodermal, endodermal, and mesodermal genes prior to neurogenesis. J Neurosci Res 2002;69:908–917.

49 Hori J, Ng TF, Shatos M et al. Neural progenitor cells lack immunogenicity and resist destruction as allografts. STEM CELLS 2003; 21:405–416.

50 Klassen H, Imfeld KL, Ray J et al. The immunological properties of adult hippocampal progenitor cells. Vision Res 2003;43:947–956.

JCB-06-0405(21125)

Journal of Cellular Biochemistry 9999:1–15 (2006)

Hyaline Cartilage Formation and Enchondral Ossification Modeled With KUM5 and OP9 Chondroblasts

Tadashi Sugiki,[1,2] Taro Uyama,[1] Masashi Toyoda,[1] Hideo Morioka,[2] Shoen Kume,[3] Kenji Miyado,[1] Kenji Matsumoto,[4] Hirohisa Saito,[4] Noriyuki Tsumaki,[5] Yoriko Takahashi,[6] Yoshiaki Toyama,[2] and Akihiro Umezawa[1]*

[1]Department of Reproductive Biology and Pathology, National Institute for Child and Health Development, Tokyo 157-8535, Japan
[2]Department of Orthopaedic Surgery, Keio University School of Medicine, Tokyo 160-8582, Japan
[3]Division of Stem Cell Biology, Department of Regeneration Medicine, Institute of Molecular Embryology and Genetics, Kumamoto University, Kuhonji, Kumamoto 862-0976, Japan
[4]Department of Allergy & Immunology, National Research Institute for Child Health and Development, Tokyo, Japan
[5]Department of Orthopaedics, Osaka University Graduate School of Medicine, 2-2 Yamadaoka, Suita, Osaka 565-0871, Japan
[6]Mitsui Knowledge Industry, Co, Ltd, Harmony Tower 21st Floor, 1-32-2 Honcho, Nakano-ku, Tokyo 164-8721, Japan

Abstract What is it that defines a bone marrow-derived chondrocyte? We attempted to identify marrow-derived cells with chondrogenic nature and immortality without transformation, defining "immortality" simply as indefinite cell division. KUM5 mesenchymal cells, a marrow stromal cell line, generated hyaline cartilage in vivo and exhibited enchondral ossification at a later stage after implantation. Selection of KUM5 chondroblasts based on the activity of the chondrocyte-specific cis-regulatory element of the collagen α2(XI) gene resulted in enhancement of their chondrogenic nature. Gene chip analysis revealed that OP9 cells, another marrow stromal cell line, derived from macrophage colony-stimulating factor-deficient osteopetrotic mice and also known to be niche-constituting cells for hematopoietic stem cells expressed chondrocyte-specific or -associated genes such as type II collagen α1, Sox9, and cartilage oligomeric matrix protein at an extremely high level, as did KUM5 cells. After cultured OP9 micromasses exposed to TGF-β3 and BMP2 were implanted in mice, they produced abundant metachromatic matrix with the toluidine blue stain and formed type II collagen-positive hyaline cartilage within 2 weeks in vivo. Hierarchical clustering and principal component analysis based on microarray data of the expression of cell surface markers and cell-type-specific genes resulted in grouping of KUM5 and OP9 cells into the same subcategory of "chondroblast," that is, a distinct cell type group. We here show that these two cell lines exhibit the unique characteristics of hyaline cartilage formation and enchondral ossification in vitro and in vivo. J. Cell. Biochem. 9999: 1–15, 2006.

Key words: Hyaline cartilage; chondroblasts; enchondral[Q2]ossification; bioinformatics; gene chip

This article contains supplementary material, which may be viewed at the Journal of Cellular Biochemistry website at http://www.interscience.wiley.com/jpages/0730-2312/suppmat/index.html.

Grant sponsor: Research on Health Science focusing on Drug Innovation (KH71064) from the Japan Health Science Foundation; Grant sponsor: The program for promotion of fundamental Studies in Health Science of the Pharmaceuticals and Medical Devices Agency (PMDA); Grant sponsor: The Ministry of Education, Culture, Sports, Science, and Technology (MEXT) of Japan; Grant sponsor: The Health, Labour Sciences Research Grants; Grant sponsor: The Pharmaceuticals and Medical Devices Agency; Grant sponsor: The research Grant for Cardiovascular Disease (H16C-6) from the ministry of Health, Labour and Welfare; Grant sponsor: Grant for Child Health and Development (H15C-2) from the Ministry of Health, Labour and Welfare.

*Correspondence to: Akihiro Umezawa, MD, PhD, Department of Reproductive Biology and Pathology, National Research Institute for Child Health and Development, 2-10-1, Okura, Setagaya, Tokyo 157-8535, Japan.
E-mail: umezawa@1985.jukuin.keio.ac.jp

Received XXXXXX[Q1]; Accepted XXXXXX

DOI 10.1002/jcb.21125
Published online 00 Month 2006 in Wiley InterScience (www.interscience.wiley.com).

The concept of regenerative medicine refers to the cell-mediated restoration of damaged or diseased tissue, and practically, regeneration of bone and cartilage may be one of the most accessible approaches. Candidate cell sources for regeneration of tissue include embryonic stem cells, fetal cells, or adult cells such as marrow stromal cells [Bianco and Robey, 2000], each of which has both benefits and drawbacks. Multipotent mesenchymal stem cells proliferate extensively, and to maintain the ability to differentiate into multiple cell types such as osteoblasts, chondrocytes, cardiomyocytes, adipocytes, and myoblasts in vitro [Umezawa et al., 1992; Pittenger et al., 1999; Bianco and Robey, 2000]. Marrow-derived stromal cells are also able to generate cardiomyocytes and endothelial cells [Makino et al., 1999], neuronal cells [Kohyama et al., 2001], and adipocytes [Umezawa et al., 1991]. Thus, marrow stromal cells are expected to be a good source of cell therapy in addition to embryonic stem cells and fetal cells [Pittenger et al., 1999].

In adults, chondrocytes maintain the extracellular matrix that gives cartilage its unique mechanical properties. Chondrocytes are long-lived and the development of new cells that are capable of producing cartilage de novo (i.e., chondroblasts) is not a normal part of adult cartilage physiology. A better understanding of the molecular mechanisms that regulate postnatal chondroblast differentiation would have a high impact on the design of strategies for cartilage repair. Cultures are commonly made from suspensions of cells dissociated from cartilage. Cartilage-derived cells in primary cultures can be removed from the culture dish and made to proliferate to form a large number of so-called secondary cultures: in this way, these cells may be repeatedly subcultured for weeks or months. Such cells often display many of the differentiated properties appropriate to their origin: the phenotype of the differentiated chondrocyte is characterized by the synthesis, deposition, and maintenance of cartilage-specific extracellular matrix molecules, including type II collagen and aggrecan [Archer et al., 1990; Hauselmann et al., 1994; Reginato et al., 1994]. The phenotype of differentiated chondrocytes is unstable in culture and is rapidly lost during serial monolayer subculturing [Benya and Shaffer, 1982; Lefebvre et al., 1990; Bonaventure et al., 1994]. This process is referred to as "dedifferentiation" and is a major impediment to the use of mass cell populations for cell therapy or tissue engineering of damaged cartilage. However, when cultured three-dimensionally in a scaffold such as agarose, collagen, or alginate, redifferentiated chondrocytes start to reexpress the chondrocytic differentiation phenotype.

This study was undertaken to obtain bone marrow-derived chondroblastic cell lines that retain critical in vivo cell functions. Previous studies showed that it was possible to obtain lines of bone marrow-derived mesenchymal stem cells, mammary gland epithelial cells, skin keratinocytes, and pigmented epithelial cells that retained critical in vivo cell functions. By implanting cells into immunodeficient mice, we identified a newly isolated KUM5 chondroblastic cell line capable of in vivo hyaline-type chondrogenesis and serendipitously found that OP9 cells derived from osteopetrotic mice and also known as a niche-constituting cells for hematopoietic stem cells had chondrogenic potential.

MATERIALS AND METHODS

Cell Culture and Chondrogenic Differentiation

The cells were cultured in the growth medium (GM): Dulbecco's modified Eagle's medium (DMEM) with high glucose supplemented with 10% fetal bovine serum for KUM5 cells; α-MEM supplemented with 10% serum (BIOWEST, lot number: S03400S1820) for OP9 cells. For chondrogenic induction of pellet culture [Johnstone et al., 1998], both KUM5 and OP9 cells were cultured in the chondrogenic medium (CM): DMEM-high glucose containing 0.1 μM dexamethasone, 1 mM sodium pyruvate, 0.17 mM ascorbic acid-2-phosphate, 0.35 mM proline, 6.25 μg/ml bovine insulin, 6.25 μg/ml transferrin, 6.25 μg/ml selenous acid, 5.33 μg/ml linoleic acid, and 1.25 mg/ml BSA (BioWhittaker). In the chondrogenic differentiation, the combination of one or several growth factors was added to the CM: TGF-β3 10 ng/ml, BMP2 50 ng/ml, BMP4 50 ng/ml, BMP6 50 ng/ml, BMP7 50 ng/ml, PDGF 50 ng/ml, hyaluronic acid 250 ng/ml. The cells and the pellets were maintained at 37°C with 5% CO_2.

Scanning Electron Microscopy (SEM) and Transmission Electron Microscopy (TEM)

The pelleted micromasses were examined by SEM and TEM. The micromasses were coated

with gold using a Sputter Coater (Sanyu Denshi Co., Tokyo, Japan) for SEM. The gas pressure was set at 50 mtorr, the current was 5 mA, and the coating time was 180 s. The samples were examined with a scanning electron microscope (JSM-6400Fs; JEOL, Ltd., Tokyo, Japan) operated at a voltage of 3 kV. For TEM, the micromasses and cell implants were initially fixed in PBS containing 2.5% glutaraldehyde for 24 h, and were embedded in epoxy resin. Ultrathin sections were double stained with uranyl acetate and lead citrate and were viewed under a JEM-1200EX transmission electron microscope (JEOL, Ltd.).

Flow Cytometric Analysis

Flow cytometric analysis was performed as previously described [Ochi et al., 2003; Mori et al., 2005; Terai et al., 2005].

Preparation and Transfection of Plasmid

The Venus gene (gift from Miyawaki) was obtained by BamHI and NotI digestion of Venus/pCS2 [Nagai et al., 2002]. The Venus gene was then cloned between the BamHI and NotI sites of pBluescriptII SK (−), excised by SalI and NotI digestion, and inserted between the XhoI and NotI sites of the p742-LacZ plasmid [Tsumaki et al., 1996], from which the LacZ gene was excised by XhoI and NotI digestion. This was named p742-Venus-Int plasmid. Transfection was performed using LipofectAmine 2000 (Invitrogen) according to the manufacturer's instructions.

Isolation of KUM5 Chondroblast

Cells were transfected with p742-Venus-Int plasmid and were cultured for 72 h. Venus-positive cells were sorted using the cell sorter (EPICS ALTRA, Beckman Courter).

In Vivo Cell Implantation Assay

To determine the ability of cultured cells to differentiate in vivo, freshly scraped cells ($2-3 \times 10^7$ cells) were subcutaneously inoculated into Balb/c nu/nu mice (Sankyo Laboratory, Hamamatsu, Japan) as previously described [Umezawa et al., 1992]. Animals were sacrificed by cervical dislocation between 1 and 8 weeks after inoculation. The subcutaneous specimens were dissected at various times after implantation and fixed and decalcified for 1 week in 10% EDTA (pH 8.0) solution. After dehydration in ascending concentrations of ethanol and xylene, the implants were embedded in paraffin. The paraffin sections were then deparaffinized, hydrated, and stained with hematoxylin and eosin, alcian blue, or toluidine blue. Paraffin sections were immunohistochemically stained with anti-type II collagen antibodies (Daiichi Fine Chemical Co., Ltd., Tokyo, Japan, Product No. F-57).

All animals received humane care in compliance with the "Principles of Laboratory Animal Care" formulated by the National Society for Medical Research and the "Guide for the Care and Use of Laboratory Animals" prepared by the Institute of Laboratory Animal Resources and published by the US National Institutes of Health (NIH Publication No. 86–23, revised 1985). The operation protocols were accepted by the Laboratory Animal Care and Use Committee of the Research Institute for Child and Health Development (2003–002).

Gene Chip Expression Analysis

Mouse-genome-wide gene expression was examined with the Mouse Genome MOE430A Probe array (GeneChip, Affymetrix), which contains the oligonucleotide probe set for approximately 23,000 full-length genes and expressed sequence tags (ESTs), according to the manufacturer's protocol (Expression Analysis Technical Manual and GeneChip small sample target labeling Assay Version 2 technical note. http://www.affymetrix.com/support/technical/index.affx). Total RNA was isolated with an RNeasy mini-kit (Qiagen, Chatsworth, CA). Double-stranded cDNA was synthesized, and the cDNA was subjected to in vitro transcription in the presence of biotinylated nucleoside triphosphates. The biotinylated cRNA was hybridized with a probe array for 16 h at 45°C, and the hybridized biotinylated cRNA was stained with streptavidin-PE and scanned with a Hewlett–Packard Gene Array Scanner. The fluorescence intensity of each probe was quantified by using the GeneChip Analysis Suite 5.0 computer program (Affymetrix). The expression level of a single mRNA was determined as the average fluorescence intensity among the intensities obtained with 11 paired (perfect matched and single nucleotide-mismatched) probes consisting of 25-mer oligonucleotides. If the intensities of mismatched probes was very high, gene expression was judged to be absent (A), even if high average fluorescence was obtained with the GeneChip Analysis Suite 5.0 program. The